eJSE International

Electronic Journal of Structural Engineering, 7(2007)

Design aspects of steel I-girders with corrugated steel webs

Ezzeldin Yazeed Sayed-Ahmed
Professor, Structural Engineering Department, Ain Shams University, Egypt. eysahmed@link.net

ABSTRACT: Corrugated web girders represent a new structural system emerged in the past two decades. The girder's flanges provide the flexural strength of the girder with no contribution from the corrugated web which provides the girder's shear capacity. Failure of the web occurs by steel yielding, web buckling or interactively between them. Lateral torsion and local flange buckling of corrugated web girders represent another two possible failure criteria. Here, the work previously performed by the author on corrugated web girders was compiled and presented in a comprehensive format. The starting point is the shear behaviour of the corrugated webs which is investigated focusing on the failure modes affecting the web design. An interaction equation that considers web buckling and yielding is proposed. Numerical analyses are performed to investigate the buckling modes of the corrugated web, verify the validity of the proposed equation and explore the post-buckling strength of corrugated web girders. The numerical model is extended to determine the critical moment causing lateral instability for corrugated web girders. The applicability of the critical moment design equations, currently used for plane web girders, to corrugated web girders is examined. The numerical model is then used to scrutinize the local buckling behaviour of the compression flange. The applicability of the currently used limiting values for the flange outstand-to-thickness ratios to corrugated web girders is investigated.

1 INTRODUCTION

Corrugated steel webs were recently used to replace the stiffened steel webs of plate/box girders (Cheyrezy & Combault 1990, Combault et al. 1993, Reinhard 1994, Lebon 1998, Combault 1988, Sayed-Ahmed 2001, 2003c, 2005c). The commonly used corrugation profile for corrugated web plates is the trapezoidal profile (Fig. 1).

The flexural strength of a steel girder with a corrugated web plate is provided by the flanges with almost no contribution from the web and with no interaction between flexure and shear behaviour. The corrugated steel web solely provides the shear capacity of the girders where the shear strength is controlled by buckling and/or steel yielding of the web. The flanges provide boundary supports for the web which lie somewhere between a simply supported boundary and a clamped one (Luo & Edlund 1994, Elgaaly et al. 1996, Johnson & Cafolla 1997a, Yoda et al. 1994).

Failure of a corrugated steel web plate occurs by the classical steel yielding of the web under a pure shear stress state. It may also occur by web buckling due to either local instability of any "panel" between two folds or overall instability of the web over two or more panels. An interactive failure mode between these different failure criteria represents another pos-

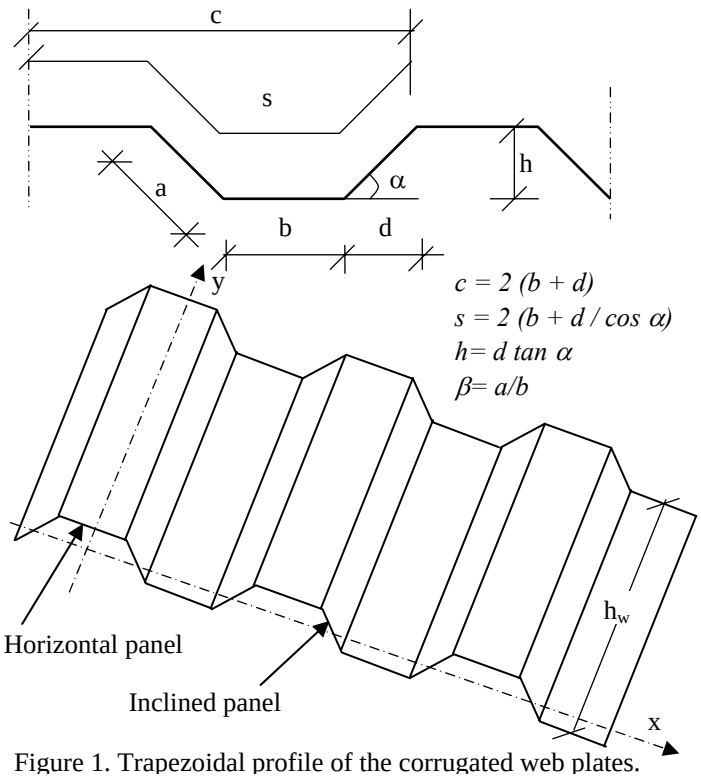

Figure 1. Trapezoidal profile of the corrugated web plates.

sibility of failure (El-Metwally 1999, Sayed-Ahmed 2001, 2005a).

Lateral torsion buckling is another possible failure mode for steel I-girders with corrugated web. Codes of practice commonly use the critical moment of a simply supported I-girder with a plane web subject to a constant moment and relate it to the critical moment of any other loading case via an "equivalent moment factor". Can the same concept still be used for corrugated web girders?

Local buckling of the compression flange of I-girders with corrugated webs is another criterion which affects design and strength of these girders. Generally, local buckling of the compression flange of an I-section mainly depends on the flange outstand-to-thickness ratio. Limits are placed on this ratio such that the critical stress initiating local flange buckling will not be reached before reaching the yield stress. Will the same limits adopted for steel girders with plane webs still be applicable to steel girders with corrugated webs? And what would be the value of the flange outstand for corrugated web girders?

This paper brings together the author previous investigations [Sayed-Ahmed 2001, 2003b, 2005a] in a comprehensive format. The different buckling modes of corrugated steel webs which may be encountered for these plates are presented and the interaction between these modes is inspected. The interaction between the yield failure criterion and the buckling modes is investigated. An interaction equation which considers the different corrugated web failure criteria is proposed. A linear finite element model is adopted to investigate the buckling modes of the corrugated web plates. Then, a nonlinear model which considers both the geometric and the material nonlinearities is employed to verify the validity of the proposed interaction equation and to investigate the post-buckling strength (if any) of the corrugated web girders.

Lateral torsion and local flange buckling of I-girders with corrugated steel webs are also numerically investigated. A finite element model is adopted to determine the critical moment initiating lateral torsion buckling of corrugated web girders and compare it to that of girders with plane webs. Corrugated web girders subjected to constant moments are first scrutinized. Then, the analysis is extended to investigate the critical moments for girders subjected to end moments causing moment gradient through the girder's span. Other corrugated web girders subjected to central concentrated loads at, and away from the shear centre are also analyzed. In evaluating the critical moment for a corrugated web girder, a section with a plane web having a proposed equivalent thickness is suggested to handle the critical moment calculations: an assumption which is verified using the numerical analysis. The validity of the equivalent moment factor concept established earlier for plane web girders is verified for corrugated web girders via the numerical analysis results. The numerical model is also used to investigate the local buckling behaviour of the compression flange for these girders. The applicability of the limits defining the section class for girders with plane web to corrugated web girders is examined.

2 FAILURE MODES OF THE CORRUGATED STEEL WEBS

The corrugated steel web solely provides the shear capacity of the girder. The shear strength is thus, controlled by buckling and/or yielding of the web (Sayed-Ahmed 2001, Luo & Edlund 1994, Elgaaly et al. 1996, Bergfelt & Leiva-Aravena 1984, Leiva-Aravena 1987, El-Metwally & Loov 1999). The only significant stress which appears in the corrugated web is pure shear stress.

2.1 *Steel Yielding of the Corrugated Web*

The shear stress which causes an element of a corrugated web to yield is defined by:

$$\tau_y = \frac{F_y}{\sqrt{3}} \tag{1}$$

where F_y is the yield strength of the steel.

2.2 *Stability of the Corrugated Web*

Two buckling modes are associated with corrugated steel webs: local buckling and overall (global) buckling. The local buckling mode corresponds to the instability of a panel simply supported between two folds. The corrugated web, in this mode of failure, acts as a series of flat panels that mutually support each other along their vertical (longer) edges. The panels are supported by the flanges along their horizontal (shorter) edges. Local buckling is investigated using equations derived for isotropic plates; an estimate for the elastic critical shear stress $\tau_{cr,l}$ for the local buckling mode is given by (Galambos 1998):

$$\tau_{cr,l} = k_s \cdot \frac{\pi^2 \cdot E}{12 \cdot (1-\upsilon^2)} \cdot \left(\frac{t_w}{b}\right)^2 \tag{2}$$

$$k_s = 5.34 + 4.0\left(\frac{b}{h_w}\right)^2 \tag{3}$$

where t_w is the corrugated web thickness, b is the panel width, E and v are Young's modulus and Poisson's ratio for the steel respectively and k_s is a shear

buckling coefficient for the local buckling mode. The shear buckling coefficient defined by Equation 3 is applicable when all the sides of the panels are simply supported which simulates steel girders with corrugated webs. In Equation 2, if the "inclined" panel width a is larger than the "horizontal" panel width b, it should be considered as the critical width.

Global (overall) buckling is characterized by diagonal buckling over several corrugation panels. The critical shear stress for this mode is estimated by considering the corrugated web as an orthotropic plate. The critical shear stress of this mode $\tau_{cr,g}$ is defined by (Galambos 1998):

$$\tau_{cr,g} = k_g \cdot \frac{\left(D_y \cdot D_x^3\right)^{1/4}}{h_w^2 \cdot t_w} \tag{4}$$

where k_g is the global shear buckling coefficient which depends solely on the web top and bottom constraints: k_g is 36 for steel girders (Luo & Edlund 1994, Johnson & Cafolla 1997a, Sayed-Ahmed, 2001, 2005a). The factors D_x and D_y are the flexural stiffness per unit corrugation about the x- and the y-axes respectively (Figure 1). These factors are defined as follows:

$$D_x = \frac{EI_x}{c} = \frac{E}{b+d}\left(\frac{bt_w[d\tan\alpha]^2}{4} + \frac{t_w[d\tan\alpha]^3}{12\sin\alpha}\right)$$
$$D_y = \left(\frac{c}{s}\right)\left(\frac{Et_w^3}{12}\right) = \left(\frac{b+d}{b+d/\cos\alpha}\right)\left(\frac{Et_w^3}{12}\right) \tag{5}$$

where I_x is the second moment of area of one *"wavelength"* of the web having a projected length c and an actual length s, t_w is the web thickness, b is the panel width, d is the horizontal projection of the inclined panel width and α is the corrugation angle.

2.3 *Interaction between Failure Modes*

The following equation is currently adopted to account for the interaction between the two buckling modes described earlier (Elgaaly et al. 1996, Johnson & Cafolla 1997a):

$$\frac{1}{\tau_{cr,i}} = \frac{1}{\tau_{cr,l}} + \frac{1}{\tau_{cr,g}} \tag{6}$$

where $\tau_{cr,i}$ is the critical stress due to the interaction between local and global buckling modes. Equation 6 does not consider the steel yielding criterion or its interaction with the buckling failure criteria. Furthermore, Equations 2 and 4 defining $\tau_{cr,l}$ and $\tau_{cr,g}$ respectively do not account for inelastic buckling which may occur if the critical shear stress of any mode exceeds $0.8\cdot\tau_y$. To overcome these defects, the following equation was proposed (Elgaaly et al. 1996, Galambos 1998) for the inelastic critical stress $\tau_{cr,in}$ in both the local and global buckling modes:

$$\begin{aligned} &\text{for } \tau_{cr,l} > 0.8\tau_y: && \tau_{cr,in,l} = \sqrt{0.8\tau_{cr,l}\tau_y} && \text{where } \tau_{cr,in,l} \le \tau_y \\ &\text{for } \tau_{cr,g} > 0.8\tau_y: && \tau_{cr,in,g} = \sqrt{0.8\tau_{cr,g}\tau_y} && \text{where } \tau_{cr,in,g} \le \tau_y \end{aligned} \tag{7}$$

To calculate the critical stress for an inelastic interactive buckling mode, $\tau_{cr,in,l}$ and $\tau_{cr,in,g}$ are used in Equation 6 instead of $\tau_{cr,l}$ and $\tau_{cr,g}$ respectively.

Another interaction equation which includes all the failure criteria has been proposed [Sayed-Ahmed 2001, 2005a, El- Metwally & Loov 1999). The new equation takes the form:

$$\left(\frac{1}{\tau_{cr,i}}\right)^n = \left(\frac{1}{\tau_{cr,l}}\right)^n + \left(\frac{1}{\tau_{cr,g}}\right)^n + \left(\frac{1}{\tau_y}\right)^n \tag{8}$$

where τ_y, $\tau_{cr,l}$ and $\tau_{cr,g}$ are defined by Equations 1, 2 and 4 respectively. A low value for the exponent n (e.g. n = 1.0) results in $\tau_{cr,i}$ being considerably less than the least of the three limits. On the other hand, higher values for n will bring $\tau_{cr,i}$ closer to the least of the three limits. A value for n of 3.0 was recently recommended (Sayed-ahmed 2005a).

Using Equations 1 to 5 and 8, typical critical shear stress curves for a trapezoidal corrugated web of steel I-girders are plotted in Figures 2 and 3. Design charts and investigation on the failure modes of

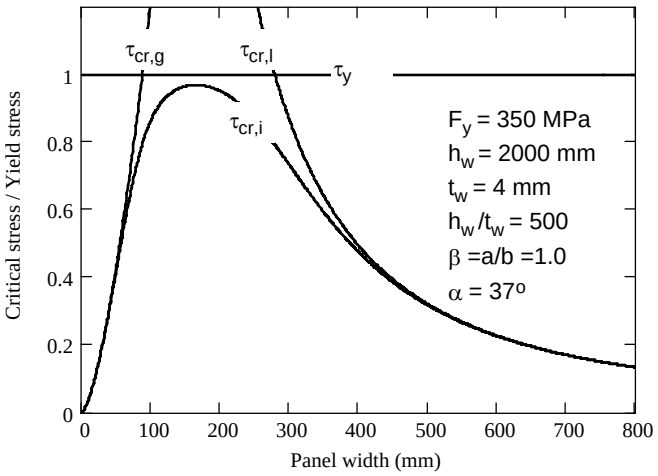

Figure 2. Critical shear stresses for trapezoidal corrugated web plates with h_w/t_w = 500 (h_w =2000 mm and t_w= 4 mm).

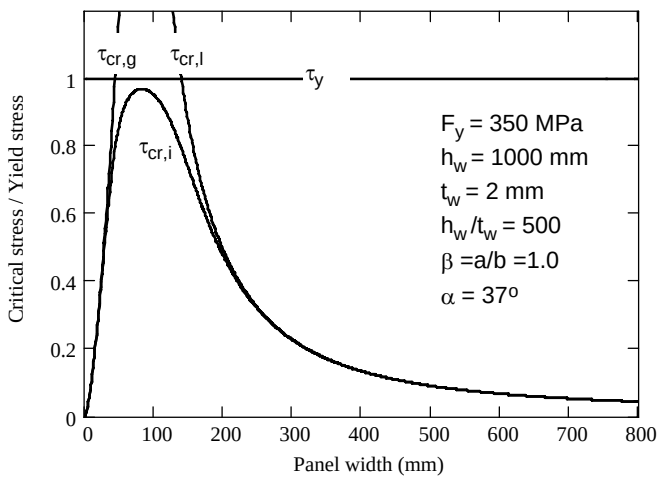

Figure 3. Critical shear stresses for trapezoidal corrugated web plates with h_w/t_w = 500 (h_w=1000 mm and t_w=2mm).

these girders are presented elsewhere (Sayed-Ahmed 2001, 2005a). Figures 2 and 3 reveal that, unlike traditional flat webs, the behaviour is not uniquely governed by the web height-to-thickness ratio (h_w/t_w).

2.4 *Numerical Modelling and Analysis*

Numerical analysis of I-girders with corrugated webs was performed using the finite element technique via the computer package ANSYS (Sayed-Ahmed 2005 a). A linear finite element model was first adopted to assess the web buckling modes using Eigenvalue analysis. A nonlinear finite element model which considered both the geometric and the material nonlinearities was then developed to investigate the validity of the proposed interaction equation (Equation 8). Isoparametric 8-node shell elements were used to model both the flanges and the corrugated web of the analyzed girders.

The numerical analyses were performed on girders which have 20 mm thick steel flanges and a web height-to-thickness ratio of 250. Different panel widths were adopted in the analyses which ranged between 20 mm and 400 mm. These panel widths correspond to panel width to web height ratios ranging between 0.04 and 0.8. The dimensions and the geometric characteristics of the analyzed girders are listed in Table 1.

Table 1. Numerically analyzed corrugated web girders.

Girder No.	G1	G2	G3	G4	G5
b (mm)	400	300	200	100	20
t_w (mm)	2	2	2	2	2
h_w (mm)	500	500	500	500	500
b/ h_w	0.8	0.6	0.4	0.2	0.04
h_w /t_w	250	250	250	250	250
b_{fl} (mm)	300	300	300	150	50
t_{fl} (mm)	20	20	20	20	20
L (span)	10.48	7.86	5.24	4.06	2.252

The geometry and loading configurations of these girders are shown in Figure 4 together with the steel uniaxial stress-strain relation adopted in the nonlinear analysis. Stiffener plates 20 mm thick were added at the loading and the support locations for all the analyzed girders. The girders were simply supported and subjected to mid-span loads (line loads acting on the top flanges as shown in Figure 5). Thus, the shear force acting on the web V is:

$$V = \tau \cdot h_w \cdot t_w \tag{9}$$

where τ is the shear stress acting on the web. Due to symmetry, only one half of the girder was analyzed with a plane of symmetry located at the girder centre-line. To eliminate the mesh sensitivity effect, the finite element analyses were first performed using

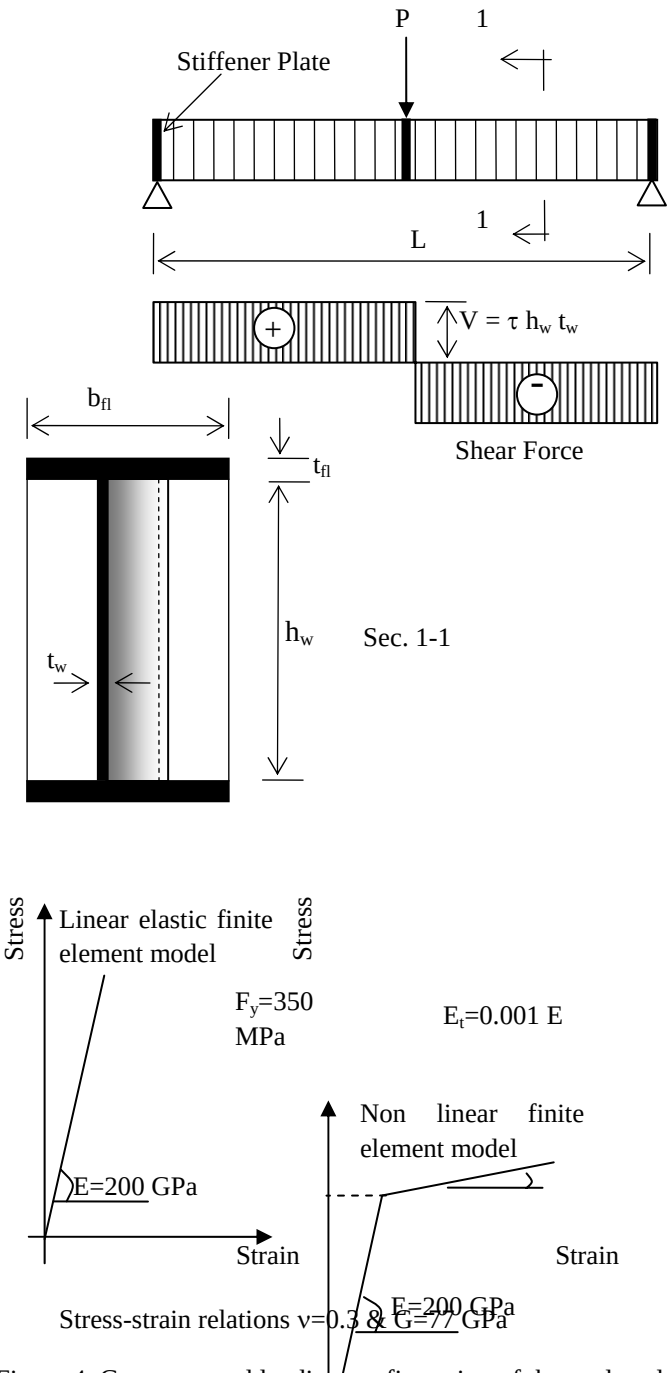

Figure 4. Geometry and loading configuration of the analyzed (above); and material model adopted in the analysis (below).

different element sizes. The typical meshes shown in Figure 5 proved to be mesh-independent.

The critical load at which web buckling was first encountered was determined in both the Eigenvalue and the nonlinear analyses. The results of the numerical analyses are plotted in Figure 6 where the ratio between shear force V_{cr} at which web buckling initiated (obtained numerically and analytically) to the shear force causing steel yielding V_y ($\tau_y h_w t_w$) is plotted versus the panel width b. Figure 6 shows that the results of the numerical analyses are in a good agreement with the behaviour theoretically predicted by the proposed interaction equation (Eq. 8). Furthermore, the results of the numerical analyses reveal that Equations 6 and 7 are conservative compared with the proposed interaction equation. Local,

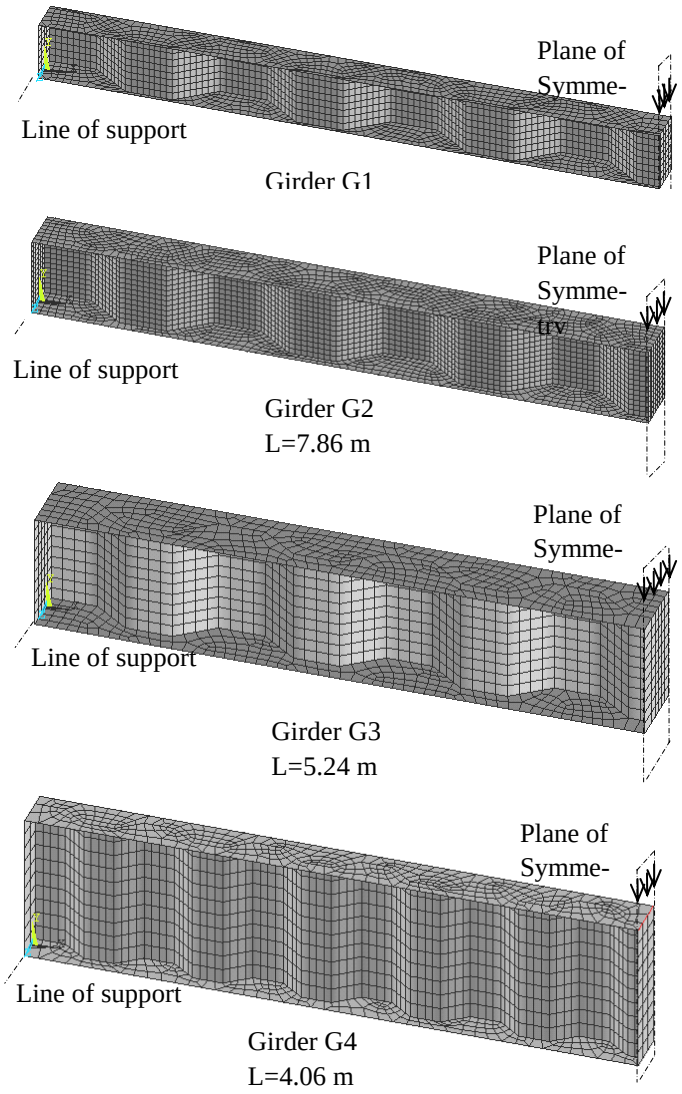

Figure 5. Typical finite element meshes adopted in the analysis (Girders are plotted in different scales).

global or interactive buckling mode was specified by inspecting the deformed shape resulting from the analysis: Figure 7 shows local and global buckling modes for Girders G3 and G5 respectively. For girders G3, the deformed shapes shown in Figure 7 were obtained from two numerical analyses; one having a finer mesh than the other: the critical loads differ by less than 1.5%.

2.5 *Post-Buckling Strength*

The nonlinear finite element model investigated the post-buckling strength (if any) of corrugated web girders (Sayed-Ahmed 2005a). To overcome the numerical difficulty resulting from the snap-through and the snap-back convergence problems which are associated with the buckling behaviour, an arc-length iterative algorithm was adopted for the incremental iterative procedures. The results revealed that girders with corrugated webs continue to carry loads after web buckling is encountered. The critical shear force V_{cr} at which web buckling was first encountered and the ultimate shear force V_{ult} at which final failure occurred are plotted in Figure 8 versus

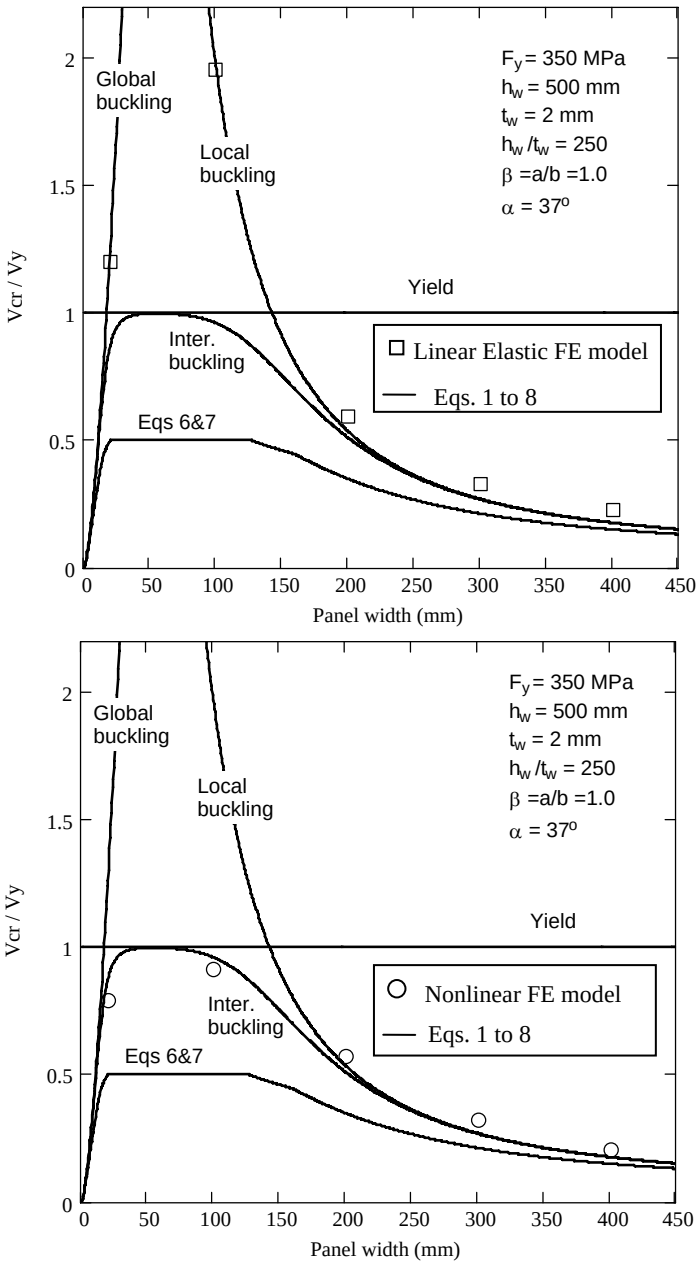

Figure 6. Critical loads determined analytically and numerically based on eigenvalue buckling analysis (above) and nonlinear finite element analysis (below).

the web panel width. The post-buckling strength $(V_{ult} - V_{cr})/V_{ult}$ is plotted in Figure 9.

It is evident from Figures 8 and 9 that the post-buckling strength of corrugated web girders is highly dependant on the panel width. For corrugated webs with larger panel widths (which suffer local buckling), the post-buckling strength may reach 53% for a 400 mm panel width. For webs with smaller panel widths, particularly those suffering global buckling, the post buckling strength is not significant.

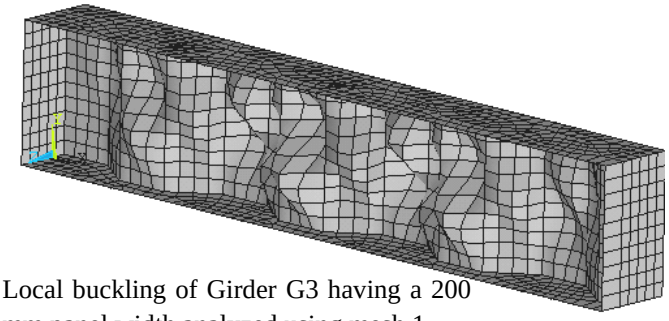

Local buckling of Girder G3 having a 200 mm panel width analyzed using mesh 1

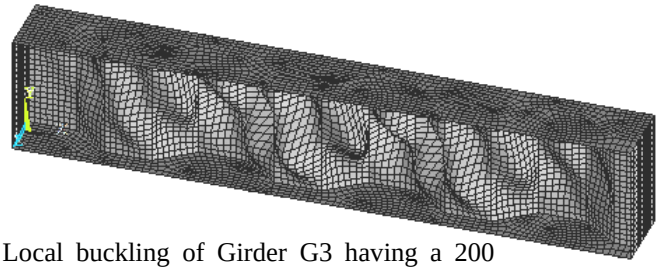

Local buckling of Girder G3 having a 200 mm panel width analyzed using mesh 2

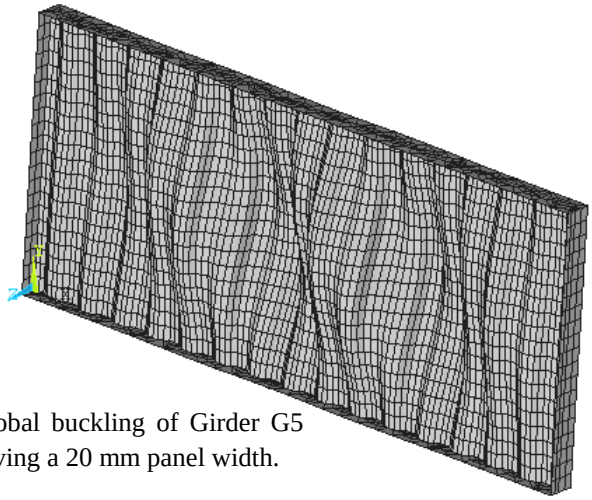

Global buckling of Girder G5 having a 20 mm panel width.

Figure 7. Buckling modes for Girders G3 and G5 resulting from the numerical analysis.

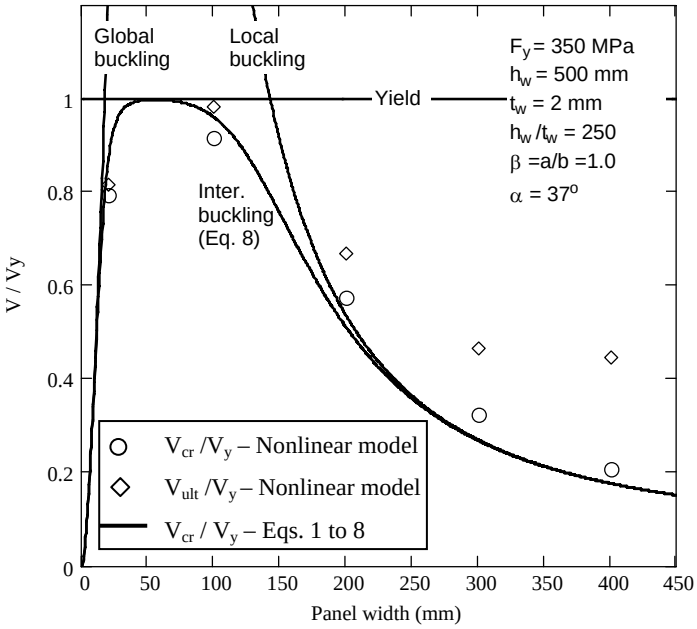

Figure 8. Critical and ultimate shear strength of the analyzed corrugated web girders.

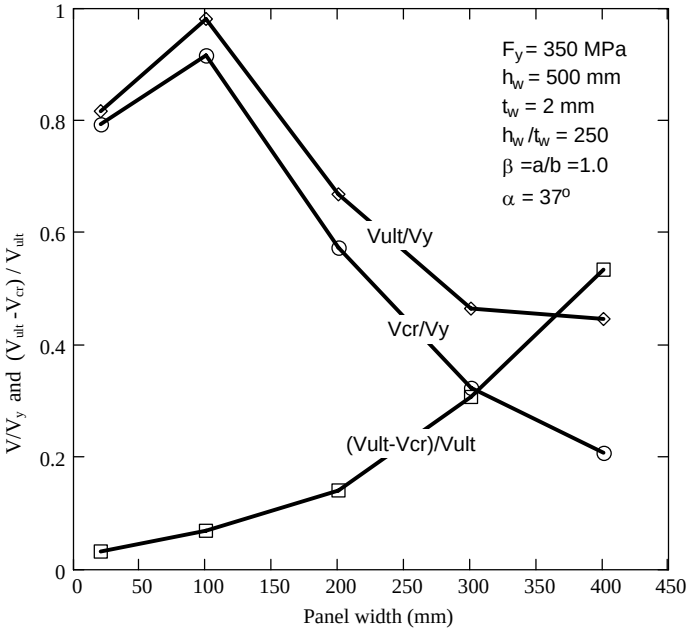

Figure 9. Post-buckling strength of the analyzed corrugated web girders.

3 LATERAL AND LOCAL FLANGE BUCKLING

3.1 *Lateral Torsion Buckling of Steel Girders with Plane Webs*

The critical moment initiating lateral instability for a simply supported I-girder is:

$$M_{cr} = C_b \cdot M_{ocr} = \frac{C_b \pi}{L} \sqrt{EI_y GJ(1 + W_R^2)} \qquad (10)$$

$$W_R = \frac{\pi}{L}\sqrt{\frac{EC_w}{GJ}} \qquad (11)$$

where M_{ocr} is the critical moment for a beam subjected to constant bending, C_b is the equivalent moment factor, E is the Young's modulus, G is the elastic shear modulus, and L is the beam span. I_y, J and C_w are the second moment of area about the weak axis of inertia, the torsional constant, and the warping constant of the beam's cross section respectively.

For beams subjected to unequal end moments (M_A and M_B) with no other loads through the beam's span, the equivalent moment factor C_b may be given by (Galambos 1998):

$$C_b = 1.75 + 1.05\frac{M_A}{M_B} + 0.3\left(\frac{M_A}{M_B}\right)^2 \qquad \leq 2.3 \qquad (12)$$

where M_A is the smaller end moment. M_A/M_B is positive for beams bent in double curvature and negative for beams bent in single curvature. CAN/CSA-S16.1-02 specifications (CSA 2002) adopted Equation 12 in design with a change in its limiting value from 2.3 to 2.5. The same specifications use C_b of

1.0 when the moment between the end supports becomes greater than the end moment or when there is no lateral support for the compression flange at one of the ends of the unsupported length. The AISC-LRFD specifications (AISC 2003) define the following equation for the equivalent moment factor:

$$C_b = \frac{12.5 \cdot M_{\max}}{3 \cdot M_1 + 4 \cdot M_2 + 3 \cdot M_3 + 2.5 \cdot M_{\max}} \qquad (13)$$

where M_1, M_2, M_3 are the absolute values of the bending moments at the quarter point, midpoint and three-quarter point of the beam, respectively and M_{max} is the maximum moment acting on the beam.

In the previous equivalent moment factor equations, the loads act along the shear centre of the beam's cross section. To include the effect of the load location with respect to the shear centre, the following definition for the equivalent moment factor C_b has been proposed (Chen and Lui 1987) and numerically verified (Sayed-Ahmed 2004):

$$C_b = \begin{cases} A/B & \text{loads acting at the top flange} \\ A & \text{loads acting at the shear centre} \\ AB & \text{loads acting at the bottom flange} \end{cases}$$

Central concentrated load:

$$A = 1.35 \qquad B = 1 + 0.649 \cdot W_R - 0.180 \cdot W_R^2 \qquad (14)$$

Uniformly distributed load:

$$A = 1.12 \qquad B = 1 + 0.535 \cdot W_R - 0.154 \cdot W_R^2$$

3.2 *Local Flange Buckling of Steel Girders with Plane Webs*

CAN/CSA-S16.1-02 specifications (CSA 2002) classify I-sections into 4 classes according to the following flange outstand-to-thickness and the web-to-thickness ratios:

$$\begin{aligned} &\text{Class 1:} && \frac{b_{fl}}{2t_{fl}} \le \frac{145}{\sqrt{F_y}} && \frac{h_w}{t_w} \le \frac{1100}{\sqrt{F_y}} \\ &\text{Class 2:} && \frac{b_{fl}}{2t_{fl}} \le \frac{170}{\sqrt{F_y}} && \frac{h_w}{t_w} \le \frac{1700}{\sqrt{F_y}} \\ &\text{Class 3:} && \frac{b_{fl}}{2t_{fl}} \le \frac{200}{\sqrt{F_y}} && \frac{h_w}{t_w} \le \frac{1900}{\sqrt{F_y}} \end{aligned} \qquad (15)$$

where $b_{fl}/2$ is the flange outstand. Classes 1 and 2 compact sections develop the fully plastic moment with higher rotation capacity of Class 1 sections. For I-sections with slender flanges or webs, local buckling may take place to the flange or the web before the fully plastic moment is developed. If local buckling occurs after developing the yield moment, then the section is classified as a Class 3 non-compact section. On the other hand, if the section can not even develop the yield moment then it is classified as a Class 4 slender section. According to the AISC-LRFD (AISC 2003), these limits are defined by:

$$\begin{aligned} &\text{Compact sections:} \\ &\frac{b_{fl}}{2t_{fl}} \le 0.38\sqrt{\frac{E}{F_y}} \qquad \frac{h_w}{t_w} \le 3.76\sqrt{\frac{E}{F_y}} \\ &\text{Non-compact sections:} \\ &\frac{b_{fl}}{2t_{fl}} \le 0.83\sqrt{\frac{E}{F_y - 69}} \qquad \frac{h_w}{t_w} \le 5.70\sqrt{\frac{E}{F_y}} \end{aligned} \qquad (16)$$

Both Class 1 and Class 2 sections of CAN/CSA-S16.1-02 specifications are considered as one class according to the AISC-LRFD (compact sections). On the other hand, the limit on Class 3 section according CAN/CSA-S16.1-02 is more restricted. For non-compact sections, the AISC-LRFD uses $F_y - 69$ in determining the yield moment to account for a residual stress of 69 MPa in case of hot-rolled steel sections (for welded sections the 69 MPa is replaced by 114 MPa).

3.3 *Lateral Torsion Buckling of Steel I-Girders with Corrugated Webs*

Lateral torsion buckling of corrugated steel web girders still need to be investigated. The critical moment causing lateral buckling was determined using a numerical model based on the finite element technique. The applicability of the equations developed for I-girders with plane webs to determine the elastic critical moment to girders with corrugated webs was examined. The applicability of the equivalent moment factor concept established for I-girders with plane webs to girders with corrugated webs was investigated using the numerical model. The effect of the point of application of the load with respect to the cross section height was scrutinized.

3.3.1 *Numerical Modelling*

Shell elements with 8 nodes and 6 degrees of freedom per node were used to model the corrugated web girders using the computer package ANSYS (Sayed-Ahmed 2003a, 2005b). The girders were considered to be simply supported in flexure and in torsion: at the beam's ends, rotation and warping about the weak axis were unconstrained while rotation about the centroidal axis was restrained. The girders were subjected to end moments with M_A/M_B ratios ranging between -1.0 and +1.0 or to a central concentrated load acting on the top flange, at the mid-height of the web or on the bottom flange. Eigenvalue buckling analysis was performed to evaluate the critical moment which initiated the lateral instability: the critical moment corresponds to the lowest eigenvalue resulting from the eigenvalue

buckling analysis. The buckling analysis was performed on girders having the cross sections shown in Figure 10. The span of all the analyzed girders was 11.52 m. Two panel widths for the corrugated web were adopted in the analysis: 200 mm and 400 mm, which correspond to panel width to web height ratios of 0.42 and 0.83. Web thicknesses of 2 mm and 4 mm were considered in the analysis which correspond to web height-to-thickness ratios of 120 and 240. The analyzed corrugation panel width-to-thickness ratio ranges between 50 and 200. The inclined panel of the corrugated web was assumed to have the same dimensional panel ($a=b$): a typical practical geometric configuration for the trapezoidal corrugation profile of the web. Stiffener plates 20 mm thick were added at the support locations for all the analyzed girders to prevent bearing failure of the webs at these locations. The flange width and thickness ($b_f/2t_f = 15$) as well as the web height were kept constant through the analysis. The mechanical and material properties of the girders' cross-section are listed in Table 2.

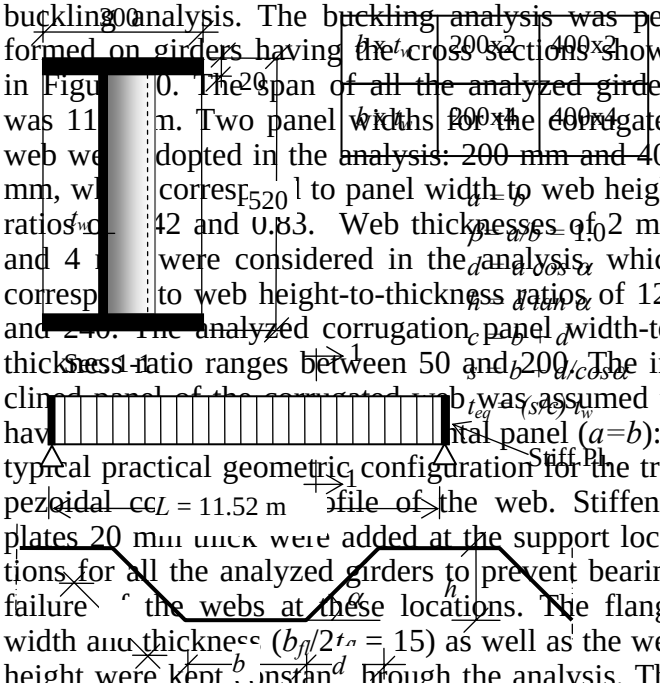

Figure 10. Geometric properties of corrugated web girders numerically analyzed for lateral torsion buckling.

Table 2. Mechanical and material properties of the analyzed corrugated web girders*.

Property	t_w =2 mm	t_w =4 mm
$A\ (10^3)\ mm^2$	13.07	14.13
$I_x\ (10^6)\ mm^4$	770.5	791
$I_y\ (10^6)\ mm^4$	90	90
r_x *mm*	243	236
r_y *mm*	83	79.8
$S_x\ (10^3)\ mm^3$	2963	3042
$S_y\ (10^3)\ mm^3$	600	600
$Z_x\ (10^3)\ mm^3$	3127	3255
$Z_y\ (10^3)\ mm^3$	900	900
$C_w\ (10^9)\ mm^3$	5625	5625
$J\ (10^3)\ mm^3$	1602	1614

*section is considered as a double symmetric I-section with an equivalent thickness $t_{eq}=s/c\ t_w$

Elastic modulus E (GPa)	Shear modulus G (GPa)	Poisson's ratio ν	Uniaxial yield strength F_y (MPa)
200	76.9	0.3	350

The theoretical critical moments of corrugated web girders subjected to constant bending moments were determined via Equation 10 to be 526.1 kN.m and 527.4 kN.m for corrugated web thicknesses of 2 mm and 4 mm respectively. It is clear that, theoretically, neither the web thickness nor the corrugation panel width of the web would have significant effect on the value of the critical moment. In these calculations, the girders were assumed to have plane webs with an equivalent thickness [13] which is given by:

$$t_{eq} = t_w \cdot s / c \tag{17}$$

where t_w is the corrugated web thickness, s is the corrugated wave length and c is the projected length of one corrugation wave (Figure 1).

Figure 11 show two typical meshes used to model two girders having corrugated panel widths of 400 mm and 200 mm, respectively. The girders were simply supported in flexure and in torsion: U_y, U_z and R_x at both ends and U_x at one of the two ends were restrained. Figure 12 shows the loading configuration considered in the analyses. For girders subjected to [illegible] the moments were applied as [illegible] are applied at the top and bottom flanges respectively at the ends of the analyzed girder. For girders subjected to concentrated loads, a point load was applied at the mid-span either on the top flange, or the bottom flange at the mid-height of the corrugated web.

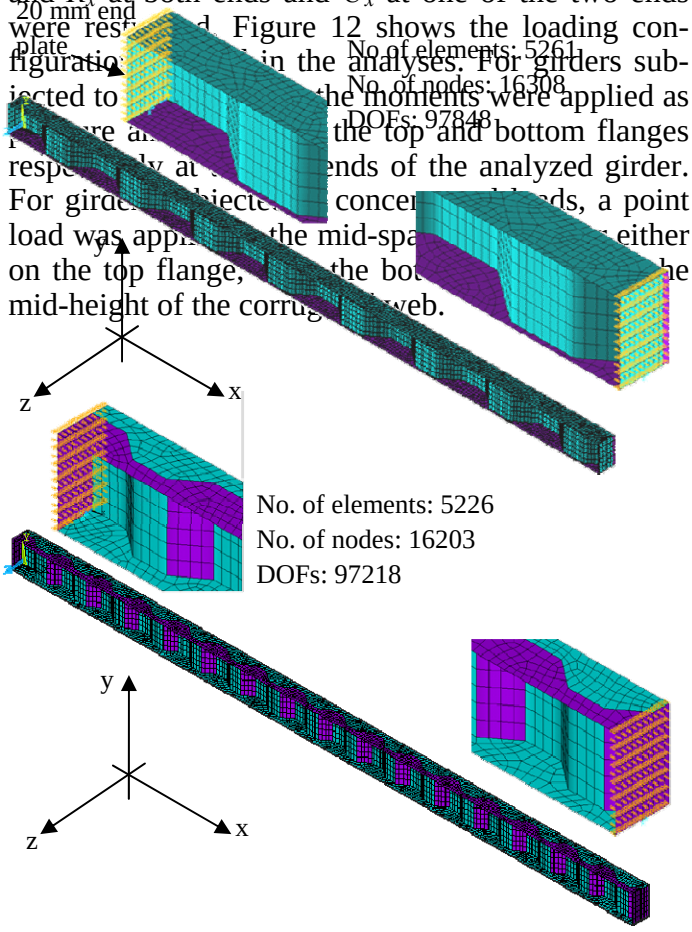

Figure 11. FE mesh for the 400 mm (above) and the 200 mm (below) corrugated web panel width girder.

3.3.2 *Results of the Numerical Analysis*

Corrugated web girders subjected to end moments or central concentrated loads (Tables 3 and 4) were numerically analyzed (Sayed-Ahmed 2003a, 2005b). Results of the numerical analysis are listed in Tables 3 and 4 and plotted in Figures 13 and 14.

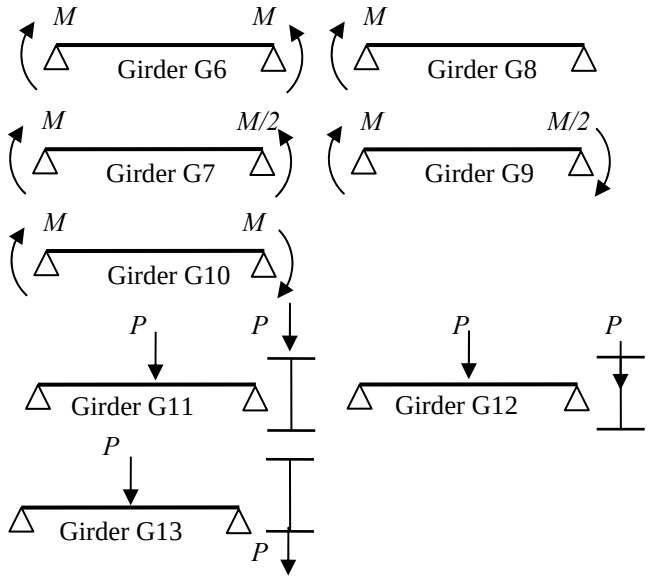

Figure 12. Loading configuration adopted in the FE analysis.

The "analytical" values of the critical moments $M_{cr\text{-}Eq.11}$ were calculated using Equation 11 with the equivalent moment factor C_b evaluated using Equation 12 for girders subjected to end moments or Equation 14 for girders subjected to concentrated loads. The theoretically calculated critical moments $M_{cr\text{-}Eq.11}$ were compared to the critical moment resulting from the numerical analysis $M_{cr\text{-}FE}$.

Table 3. Results of the finite element buckling analysis for corrugated steel web girders subjected to end moments.

Panel dim.	Girder	G6	G7	G8	G9	G10
	$C_{b\text{-}Eq.12}$	1	1.3	1.75	2.3	2.3
b = 200 mm t_w = 2 mm	$M_{cr\text{-}FE}$ (kN.m)	606	798	1098	1523*	1661*
	$C_{b\text{-}FE}$	1	1.32	1.81	2.51	2.74
	$M_{cr\text{-}FE}$ / $M_{cr\text{-}Eq\ 11}$	1.152	1.167	1.192	1.258	1.373
b = 400 mm t_w = 4 mm	$M_{cr\text{-}FE}$ (kN.m)	635.1	836	1145	1559*	1664*
	$C_{b\text{-}FE}$	1	1.31	1.8	2.45	2.62
	$M_{cr\text{-}FE}$ / $M_{cr\text{-}Eq\ 11}$	1.204	1.219	1.24	1.285	1.372

*Lateral buckling is preceded by flange and/or web local buckling mode.

Table 4. Results of the finite element buckling analysis for corrugated steel web girders subjected to central loads.

Panel dim.	Girder	G11	G12	G13
	$C_{b\text{-}Eq.13}$	1.31	1.31	1.31
	$C_{b\text{-}Eq.14}$	0.96	1.35	1.9
mm t_w =	$M_{cr\text{-}FE}$	609	848	1122
	$C_{b\text{-}FE}$	0.958	1.335	1.766
	$M_{cr\text{-}FE}$ / $M_{cr\text{-}Eq\ 11}$*	1.202	1.19	1.12

*Based on C_b from Equation 14.

The numerically obtained critical moments $M_{cr\text{-}FE}$ were also related to the critical moment of Girder G6 subjected to constant flexure through the span. Thus, equivalent moment factors for all the numerically analyzed corrugated web girders were evaluated: those are listed in Tables 3 and 4 and plotted in Figures 13 and 14 versus the equivalent moment factors analytically calculated using the currently adopted equations (Equations 12 to 14).

It is evident from Tables 3 and 4 and Figures 13 and 14 that resistance to lateral torsion buckling of girders with corrugated webs is different from that of plate girders with traditional plane webs. The critical moment initiating lateral buckling for corrugated web girders is larger than that of traditional girders. The numerical analysis reveals that M_{cr} for corrugated web girders subject to end moments is 15% to 37% higher than M_{cr} for plane web girders. This ratio becomes 12% to 20% for corrugated web girders subject to central concentrated loads.

The numerical analysis also reveal that the concept of the equivalent moment factor which is currently used for I-girders with plane web to account for the moment gradient is applicable to girders with corrugated webs. Furthermore, the analysis results show that Equations 12 and 13 which are currently used to calculate the equivalent moment factor are also applicable to steel girders with corrugated webs.

Figure 13 shows that in case of girders subjected to end moments, Equation 12 with the CAN/CSA-S16.1-02 limiting value provides a good match to the results of the numerical analysis.

The importance of the location of the applied load with respect to the shear centre of the girder's cross-section is emphasized through the results plotted in Figure 14 and listed Table 4. It is clear from these results that Equation 14 which considers the location of the load with respect to the shear centre produces a better match to the numerical analysis results compared to the currently used provisions of CAN/CSA-S16.1-02 or AISC-LRFD.

3.4 *Local Buckling of Corrugated Web girders' Compression Flanges*

The flange outstand for girders with plane webs was commonly approximately as $b_{fl}/2$. For corrugated web girders at a section where the web is parallel to the axis of the girder, there is a large outstand on one side and a small outstand on the other (Figure 15).

Thus, the flange outstand which should be used to classify the cross section class of corrugated web girders (Eq. 15 and 16) may be based on the large flange outstand L_l, the small flange outstand L_s or

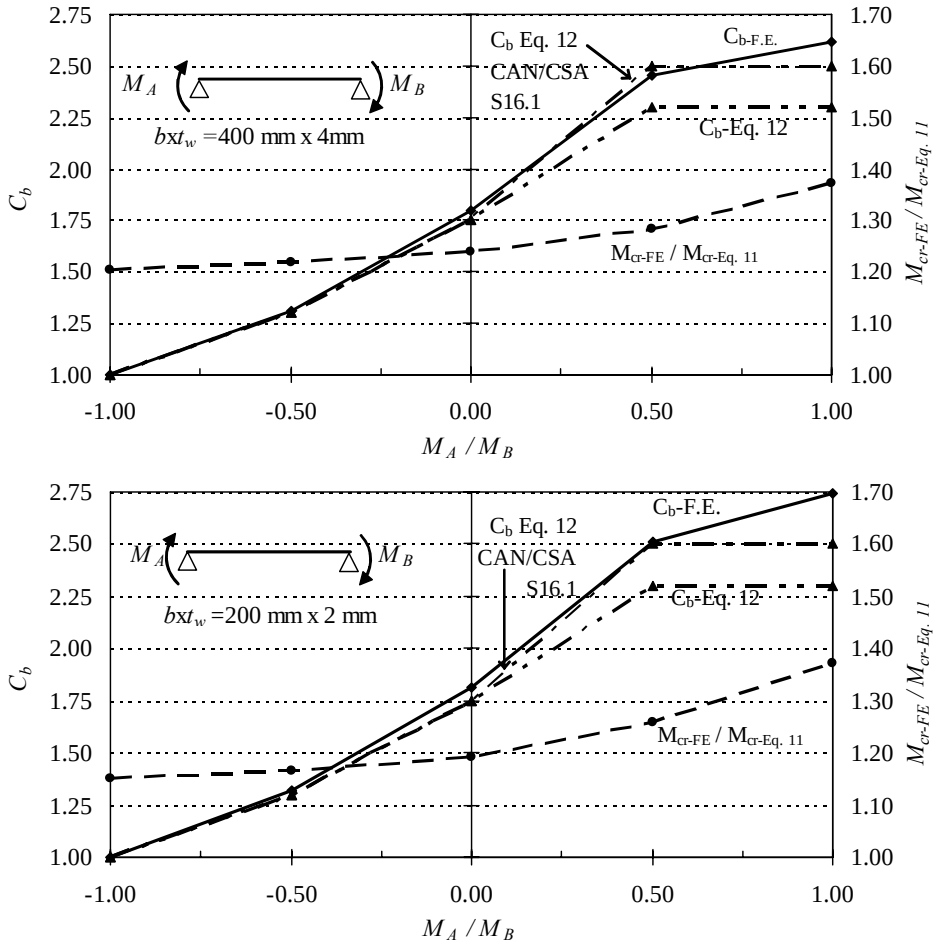

Figure 13. Equivalent moment factor and the critical moments for girders with corrugated webs subjected to end moments.

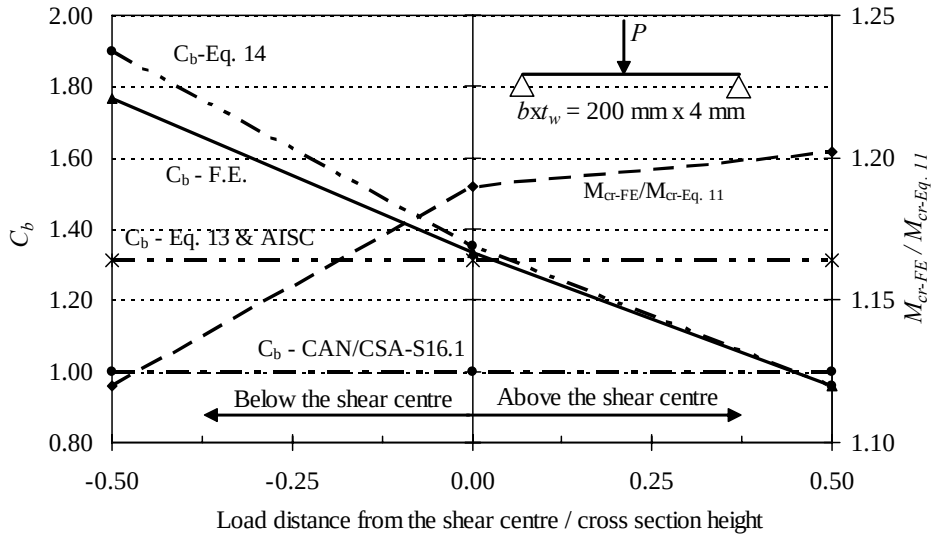

Figure 14. Equivalent moment factor for girders with corrugated webs subjected to central concentrated loads.

the average flange outstand L_{av} (Fig. 15). The average flange outstand corresponds to $b_{fl}/2$ which is traditionally used for girders with plane webs.

Based on a previous investigation (Johnson & Cafolla 1997b), it was argued that the average flange outstand L_{av} may only be used as $b_{fl}/2$ if a ratio R is less that 0.14 where R is the ratio between area EFGH and area ABCD defined in Figure 15. For R greater than 0.14, which is more practical, it is recommended to be conservative using the large flange outstand L_l. Thus, a considerable uncertainty still exists regarding the correct value which should be used for the flange outstand of corrugated web girders.

3.4.1 *Numerical Modeling*

Local buckling behaviour of the compression flange of corrugated web girders is numerically investigated (Sayed-Ahmed 2005b). The adopted finite element model is similar to the one used earlier for lateral torsion buckling. The girders were simply supported and subjected to constant moments through the span: the upper and lower flanges were subjected to states of uniform compression and uniform tension respectively. Eigenvalue analysis using the finite element package ANSYS was performed to evaluate the stress and the compressive force which caused local buckling for the upper flange (Sayed-Ahmed 2005b).

The numerical analysis was performed on corrugated web girders having the cross sections and the geometric properties shown in Figure 15 with the material properties listed in Table 2. The span of all the analyzed girders was 11.52 m. The corrugated web panel width adopted in the analysis was 200 mm. Web thicknesses of 2 mm and 4 mm were considered in the analysis which corresponds to web height-to-thickness ratios h_w/t_w of 120 and 240 and panel width to web thickness ratios b/t_w of 50 and 100 respectively. The flange width-to-thickness ratio $b_{fl}/2t_{fl}$ was varied between 7.5 and 37.5 based on the

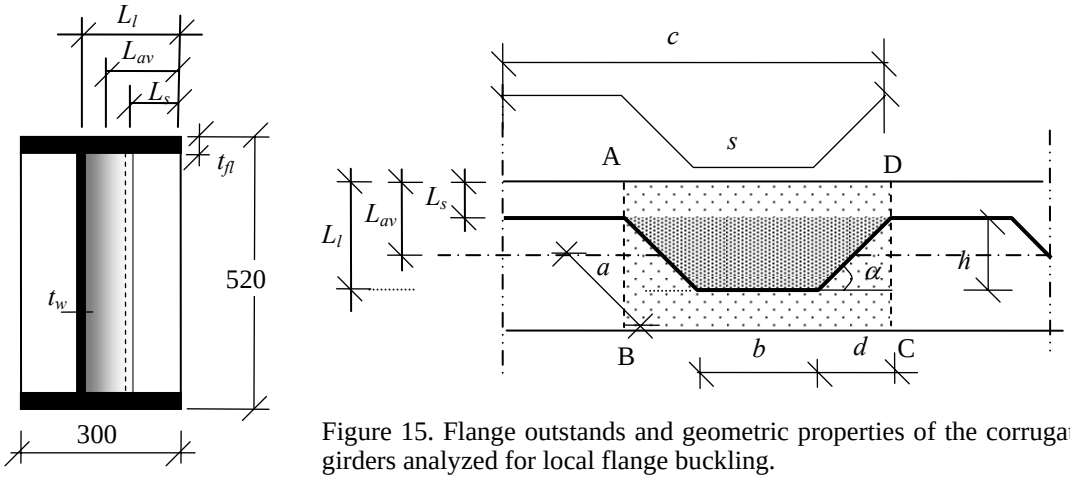

Figure 15. Flange outstands and geometric properties of the corrugated web girders analyzed for local flange buckling.

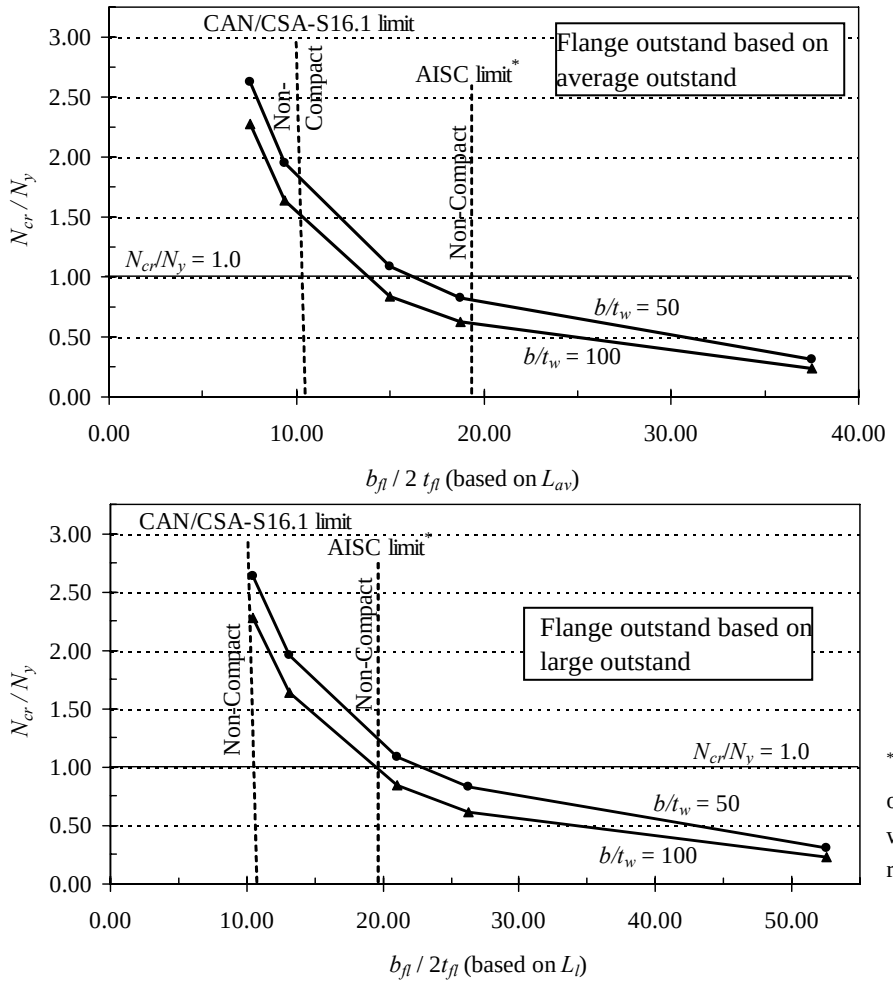

* The AISC-LRFD limit on $b_{fl}/2t_{fl}$ is calculated without considering the residual stresses

Figure 16. Local buckling of corrugated web girders' flanges and current compact section limits.

average flange outstand or 10.5 and 52.5 based on the large flange outstand. The finite element meshes used to model the girders is similar to the one shown in Figure 12 for the 200 mm panel width girder.

3.4.2 *Results of the Numerical Analysis*

The critical compressive force N_{cr} acting on the upper flange at which local flange buckling occurred was numerically determined. This force was normalized with respect to the yield strength of the flange N_y where $N_y = b_{fl}$ x t_{fl} x F_y and plotted versus the average flange outstand-to-thickness and the large flange outstand-to-thickness ratios in Figure 16. The non-compact section limits according to the AISC-LRFD and the CAN/CSA-S16.1-02 were also plotted in Figure 16. The AISC-LRFD limit on $b_{fl}/2t_{fl}$ in this figure does not consider the residual stress (69 MPa for rolled section and 114 MPa for welded sections) as the yield strength of the compression flange N_y was based on the full yield stress F_y.

Figure 16 reveals that using the average flange outstand-to-thickness ratio to classify the section of a corrugated web girder' is acceptable according to the restricted limits of the CAN/CSA-S16.1-02 specifications: $N_{cr}/N_y > 1.0$ for $b_{fl}/2t_{fl} < 10.7$ with $b_{fl}/2$ based on the average flange outstand. On the other hand, the large flange outstand-to-thickness ratio is more appropriate for classifying a corrugated web girder's cross section according to the AISC-LRFD provisions: $N_{cr}/N_y > 1.0$ for $b_{fl}/2t_{fl} < 19.8$ only when $b_{fl}/2$ is based on the large flange outstand.

The AISC-LRFD assumes that the web of a plane web I-girder provide a support condition for the flange outstand (Fig. 17) which lies somewhere between a fixed support (k=1.277) and a simple support (k=0.425). The buckling coefficient k was assumed for this hypothetical case of the AISC-LRFD to be 0.7 hence, the limit on $b_{fl}/2t_{fl}$ given in Equation 16. The critical loads causing local flange buckling for a corrugated web girder flange, obtained from the numerical analysis, were plotted in Figure 18 versus the flange large outstand-to-thickness ratio. The basic plate buckling equation with the three buckling coefficients described above were also plotted in Figure 18. The figure confirms that the flange outstand-to-thickness ratio should be based on the large outstand for girders with corrugated webs (Sayed-Ahmed 2005b). Figure 18 also reveals that the assumed value of k=0.7 which is adopted by the AISC-LRFD specifications for plane web girders is equally applicable to girders with corrugated web provided that the large outstand is used for $b_{fl}/2$.

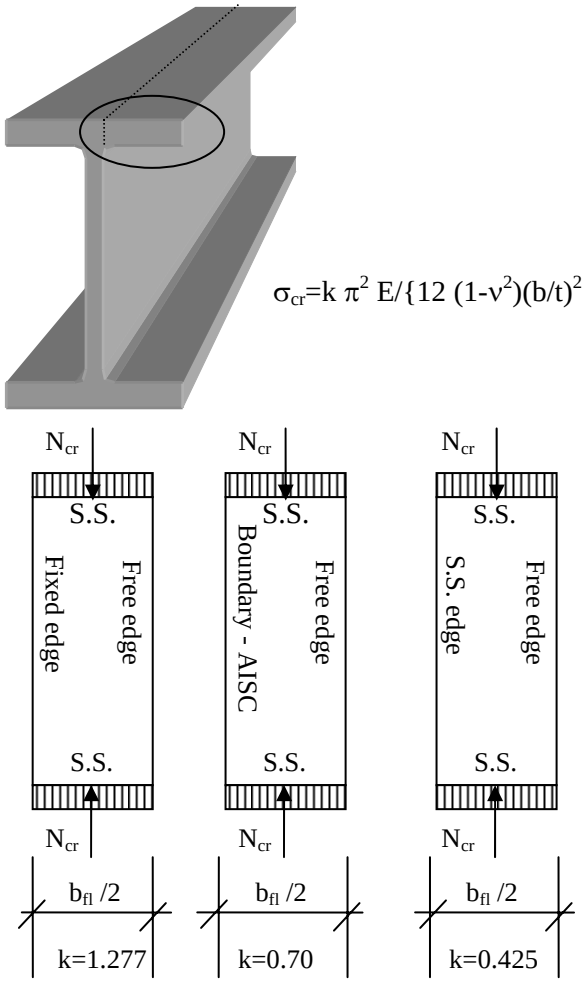

Figure 17. Simulation of local flange buckling for I-girders and modeling of the web support according to AISC-LRFD.

4 CONCLUSIONS

Corrugated webs of corrugated web girders provide the girder's shear capacity with no contribution to its moment capacity. The corrugated web is subjected to a pure shear stress state. Its behaviour is controlled by shear buckling and steel yielding. Two modes of buckling are defined for these webs: local buckling and global buckling. An interaction between the two buckling modes represents another possibility of failure. Interaction between these buckling modes and the yield failure criterion controls failure of these web plates within all practical ranges of their geometric dimensions. An interaction equation defining the interactive failure mode of the corrugated web plates is proposed. Numerical models have been developed to investigate the buckling behaviour of the corrugated web plates and to examine the validity of the proposed interaction equation. The results obtained from model were found to be in a good agreement with the prediction obtained using the proposed equation. The model was extended to investigate the post-buckling strength for corrugated web girders. The post-buckling strength was found to be highly dependent on the panel width of the corrugated webs: it varies between 3% and 53% depending on the panel width.

Lateral torsion buckling of I-girders with corrugated webs has been numerically investigated. It was concluded that resistance to lateral torsion buckling

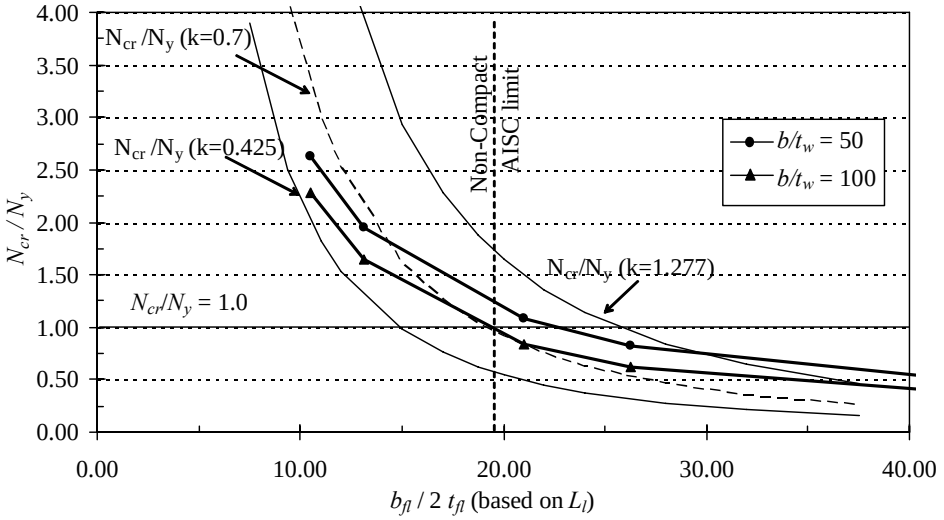

Figure 18. Local buckling of the corrugated web girders' flanges and the assumed buckling coefficients of the AISC-LRFD.

of such girders is 12% to 37% higher than that of plate girders with plane webs. Thus, the equations used to calculate the critical moment of girders with plane webs would underestimate the capacity of plate girders with corrugated web to resist lateral buckling but they are conservative for design purposes. Furthermore, it was concluded that the equivalent moment factor concept which is used for the plate girders with plane web is equally applicable to plate girders with corrugated webs. Thus, all the equations and tables which are currently used to determine the equivalent moment factor for plane web girders may be used for corrugated web girders.

The numerical model was used to investigate the local buckling of the compression flange of corrugated web girders. It is concluded that the flange outstand-to-thickness ratio, which is currently used by codes of practice as one of the criteria classifying the section compactness, should be based on the large outstand of the corrugated web girder's flange.

5 REFERENCES

American Institute of Steel Construction (AISC). 2003. Manual of steel construction: Load and Resistance Factor Design (LRFD). 3rd edition, Illinois, USA.

Bergfelt, A. and Leiva-Aravena, L. 1984. Shear buckling of trapezoidal corrugated girder webs, Division of steel and Timber Structures, Chalmers University of Technology, Gothenburg, Publication S 84:2, Sweden, 64p.

CAN/CSA-S16.1-02. 2002. Limit states design of steel structures. Canadian Standard Association, Ontario, Canada.

Capra, A. and Leville, A. 1996. The bridge at Dole, Proceedings of the FIP Symposium, Post-Tensioned Concrete Structures. London, Vol. 1, pp. 135-141.

Chen, W., and Lui, E. 1987. Structural stability: theory and implementation. Elsevier Science Publishing Co., NY, USA.

Cheyrezy, M. and Combault, J. 1990. Composite bridges with corrugated steel webs - achievement and prospects, IABSE Symposium, Mixed Structures: Including New Materials, IABSE Reports, Brussels, pp.479-484.

Combault, J. 1988. The Maupré Viaduct near Charolles, France, Proceedings of the NEC/COP National Steel Construction Conference, Miami Beach, USA, pp.12.1-12.22.

Combault, J, Lebon, J.D. and Pei, G. 1993. Box girders using Corrugated Steel Webs and Balanced Cantilever Construction. Proc. of the FIP Symposium, Kyoto, pp. 417-424.

Elgaaly, M., Hamilton, R.W. and Seshadri, A. 1996. Shear strength of beams with corrugated webs, Journal of Structural Engineering, ASCE, Vol. 122, No. 4, pp. 390-398.

El-Metwally, A.S. 1999. Prestressed Composite Girders with Corrugated Webs. MSc Thesis, Department of Civil Eng. The University of Calgary, Calgary, Alberta, Canada, 189p.

El-Metwally, A.S. and Loov, R.E. 1999. Composite prestressed concrete beams with corrugated webs, Proc. of the Annual Conference of the Canadian Society for Civil Engineering, Regina, Saskatchewan, Canada, Vol. 1, pp. 305-314.

Galambos, T.V. 1998. Guide to stability design criteria for metal structures, 5th ed., John Wiley and Sons, NY, USA.

Lebon, J. 1998. Steel corrugated web bridges - first achievements, Proc. of the 5th Int. Conf. on Short and Medium Span Bridges, CSCE, Calgary, Canada, CD-Proceedings.

Leiva-Aravena, L. 1987. Trapezoidally corrugated panels - buckling behaviour under axial compression and shear, Division of steel and Timber Structures, Chalmers University of Technology, Gothenburg, Report S84:2, Sweden, Publication S 87:1.

Luo, R. and Edlund, B. 1994. Buckling of trapezoidally corrugated panels using spline finite strip method, Thin Walled Structures, Elsevier Science Limited, Vol . 18, pp. 209-240.

Johnson, R.P. and Cafolla, J. 1997a. Corrugated webs in plate girders for bridges, Structures and Buildings, ICE, Vol 123, pp.157-164.

Johnson, R.P. and Cafolla, J. 1997b. Local flange buckling in plate girders with corrugated webs, Structures and Buildings, ICE, Vol 123, pp. 148-156.

Reinhard, J.M. 1994. Pont de la Corniche, Ouvrages d'Art No. 19, pp. 14-19 (in-French).

Sayed-Ahmed, E.Y. 2001. Behaviour of steel and/or composite girders with corrugated steel webs, Canadian Journal of Civil Engineering, vol. 28, No. 4, pp. 656-672.

Sayed-Ahmed, E.Y. 2003a. Lateral Stability of Plate Girders with Corrugated Steel Webs. Proceedings, 31st Canadian Society for Civil Engineering Conference: Building our Civilization, Moncton, New-Brunswick, Canada. June 2003. GCF231-1 to GCF231-10.

Sayed-Ahmed, E.Y. 2003b. Girders with Corrugated Steel Webs: Buckling Modes and Numerical Modeling. Proceedings, Advances in Structures: Steel, Concrete, Composite and Aluminum, Sydney, Australia, June 2003, pp. 807-812.

Sayed-Ahmed, E.Y. 2003c. Composite Bridges Constructed with Corrugated Steel Web Box Girders. Proceedings, International Symposium - Celebrating Concrete: People and Practice, University of Dundee, Dundee, Scotland (Dhir, Newlands, McCarthy, Eds), pp. 43-52.

Sayed-Ahmed, E.Y. 2004. Lateral buckling of steel I-beams: a numerical investigation and proposed equivalent moment factor equations. Al-Azhar University Engineering Journal, Vol. 7, No. 1, pp. 111-123.

Sayed-Ahmed, E.Y. 2005a. Plate girders with corrugated steel webs. AISC Engineering Journal, Vol 42, No. 1, pp. 1-13.

Sayed-Ahmed, E.Y. 2005b. Lateral Torsion-Flexure Buckling of Corrugated Web Steel Girders. Structures & Buildings, ICE, Vol. 158 (SB1), pp. 53-69.

Sayed-Ahmed, E.Y. 2005c. Innovative Steel Plate Girders with Corrugated Webs for Short Span Bridges. Proc., 4th Int. Conf. on Current and Future Trends in Bridge Design, construction and Maintenance, Institution of Civil Engineering (ICE-London, UK), Kuala Lumpur, Malaysia, Oct. 2005.

Yoda, T., Ohura, T. and Sekii, K., 1994. Analysis of Composite PC Box Girders with corrugated steel webs. Proc. of the 4th Int. Conf. on Short and Medium Span Bridges, Halifax, Nova Scotia, Canada, pp. 1107- 1115.